Is Accelerometry an Effective Method to Assess Muscle Vibrations in Comparison to Ultrafast Ultrasonography?

Robin Trama, Christophe Hautier, Robin Souron, Thomas Lapole, Alexandre Fouré, Yoann Blache

▶ **To cite this version:**

Robin Trama, Christophe Hautier, Robin Souron, Thomas Lapole, Alexandre Fouré, et al.. Is Accelerometry an Effective Method to Assess Muscle Vibrations in Comparison to Ultrafast Ultrasonography?. IEEE Transactions on Biomedical Engineering, 2021, 68 (4), pp.1409-1416. 10.1109/TBME.2020.3035838 . hal-03467157

HAL Id: hal-03467157
https://hal.science/hal-03467157v1

Submitted on 31 Aug 2023

HAL is a multi-disciplinary open access archive for the deposit and dissemination of scientific research documents, whether they are published or not. The documents may come from teaching and research institutions in France or abroad, or from public or private research centers.

L'archive ouverte pluridisciplinaire **HAL**, est destinée au dépôt et à la diffusion de documents scientifiques de niveau recherche, publiés ou non, émanant des établissements d'enseignement et de recherche français ou étrangers, des laboratoires publics ou privés.

Is accelerometry an effective method to assess muscle vibrations in comparison to ultrafast ultrasonography?

Robin Trama, Christophe A. Hautier, Robin Souron, Thomas Lapole, Alexandre Fouré, and Yoann Blache

***Abstract*— *Objective:* The purpose of this study was to assess whether accelerometry effectively reflects muscle vibrations measured with ultrafast ultrasonography. *Methods:* Vibration characteristics initiated on the *vastus lateralis* muscle by an impactor were compared when assessed with accelerometry and ultrasonography. Continuous wavelet transforms and statistical parametric mapping (SPM) were performed to identify discrepancies in vibration power over time and frequency between the two devices. *Results:* The SPM analysis revealed that the accelerometer underestimated the muscle vibration power above 50 Hz during the first 0.06 seconds post impact. Furthermore, the accelerometer overestimated the muscle vibration power under 20 Hz, from 0.1 seconds after the impact. Linear regression revealed that the thicker the subcutaneous fat localized under the accelerometer, the more the muscle vibration frequency and damping were underestimated by the accelerometer. *Conclusion:* The skin and the fat tissues acted like a low-pass filter above 50 Hz and oscillated in a less damped manner than the muscle tissue under 20 Hz. *Significance:* To eliminate some artifacts caused by the superficial tissues and assess the muscle vibration characteristics with accelerometry, it is suggested to 1) high-pass filter the acceleration signal at a frequency of 20 Hz, under certain conditions, and 2) include participants with less fat thickness. Therefore, the subcutaneous thickness must be systematically quantified under each accelerometer location to clarify the differences between subjects and muscles.**

***Index Terms*—Acceleration, Continuous wavelet transforms, Damping, Statistical parametric mapping**

I. Introduction

SOFT tissue vibrations have been widely studied for various purposes over the past three decades. The first objective of these studies was to assess the vibration characteristics, such as amplitude, main and median frequencies, and damping properties [1]–[6]. Thereafter, studies aimed to better understand muscular activity tuning in response to impact and its effect on vibration (i.e., the muscle tuning paradigm) [7]–[12]. Then, some researchers demonstrated that muscular fatigue generated an increase in the vibration amplitude [13]–[15]. Currently, there is growing interest in assessing the influence of sports equipment on the decrease of soft tissue vibrations [15]–[21]. Notably, in all the aforementioned studies, soft tissue vibrations were quantified with accelerometers attached to the skin. Although accelerometry is the most applicable method for assessing soft tissue vibrations, this approach involves the recording of the accelerations of all the soft tissue packages, namely, the skin, the subcutaneous fat, and the muscle. Considering that muscle injuries [22], [23] and fatigue [24] can be caused by vibrations, the characterization of muscle vibrations, rather than the vibrations of the overall soft tissue package, is of greater interest. A previous study reported that muscle and other soft tissues do not share the same mechanical properties [25]; therefore, soft tissue vibrations measured by accelerometry might not accurately reflect muscle vibrations.

Recently, ultrafast ultrasound devices have been used to quantify continuous vibrations of a spinal bone [26] and the quadriceps muscles vibrating at frequencies below 10 Hz [27]. Analysis of such vibrations was performed using high-frequency image recording combined with image tracking algorithms. Although the vibrations were of a lower frequency and amplitude than those usually observed during sports activities, ultrasonography is a promising tool to assess impact-induced muscle vibrations without influence from the vibrations of the other soft tissues (i.e., the skin or subcutaneous fat). To the best of our knowledge, no study has assessed whether significant differences between accelerometry and ultrasonography may be observed when estimating muscle vibrations. Nevertheless, identifying such potential discrepancies could contribute to a better characterization of muscle vibrations assessed in realistic conditions with accelerometry.

Consequently, the purpose of this study was to determine whether a skin-mounted accelerometer reflects muscle vibrations assessed with ultrafast ultrasonography in a relaxed or contracted muscle. Based on a previous study [25], we hypothesized that soft tissue vibrations assessed with an accelerometer would be of greater amplitude, of lower frequency, and with reduced damping properties than muscle vibrations assessed with ultrasonography.

II. Material and methods

A. Participants

A group of 15 participants composed of 12 men and 3 women (25.1 ± 4.4 years, 176 ± 6 cm, 70.7 ± 9.8 kg) volunteered to participate in this study. All the participants were healthy and free from lower-limb injury. The study was approved by the local university ethics committee, according to the statement of ethical principles of the Declaration of Helsinki, and the participants signed an informed consent document.

B. Instrumentation

An electromyogram (EMG) of the *vastus lateralis* of the right leg was recorded at 1000 Hz with pairs of surface electrodes (Delsys, Natick, Massachusetts, USA). An Aixplorer ultrasound device was used with an SL15-4 probe (Supersonic Imagine, Aix-en-Provence, France) to obtain video of the *vastus lateralis* vibrations (1000 Hz). The soft tissue acceleration of the thigh as well as the probe acceleration (± 50 g, 1000 Hz) were recorded with two biaxial accelerometers (Mega Electronics, Kuopio, Finland).

C. Procedure and data collection

Participants were seated on a custom-built isometric knee-extensor ergometer, with the hip and knee angles set at 90° and the chest secured with a safety belt. After having shaved and cleaned the skin with alcohol, surface electromyographic electrodes were placed on the *vastus lateralis* belly, according to SENIAM recommendations [28]. Before the experiment, participants performed a standardized warm-up consisting of ten incremental isometric knee extensions of 5 seconds. After a 3-minute rest period, participants performed two maximum voluntary isometric contractions to determine the maximal EMG signal and normalize the *vastus lateralis* activation level (see Data treatment section below).

Testing consisted of an assessment of *vastus lateralis* accelerations induced by an external shock, using a pendulum impactor (i.e., a reflex hammer was dropped from an angle of 45° with respect to the vertical). The position of the impactor was adjusted so that the impact was administered 6 cm distally from the location of the muscle-vibration measurement device. Shocks were administered under a relaxed condition (4 shocks) and a contracted condition (4 shocks at 40% of the maximal activation). Visual feedback of the 0.05-second normalized root-mean-square EMG of the *vastus lateralis* was displayed on a computer screen to help the participant achieve the 40% ± 10% target activation level. The impact was administered when the activation level was reached.

For each condition, two-dimensional *vastus lateralis* vibrations were measured with both an ultrasound device and an accelerometer. The ultrasound probe was positioned perpendicularly to the longitudinal axis of the thigh and proximally to the EMG electrodes. The position of the probe, ensuring two-dimensional analysis of the muscle vibrations along the mediolateral and anteroposterior axes of the thigh (Fig. 1), was marked on the skin, and the probe was clamped with a mechanical arm. A water-based gel was applied between the skin and the probe to avoid probe-skin contact. The position of the probe was adjusted between the relaxed and contracted conditions to keep the probe out of contact with the skin when the muscle expanded and, therefore, avoid any pressure from the probe on the skin. Once all the shocks were administered, the probe was replaced by the accelerometer, which was placed at the same location and oriented in the same direction as the probe. Thereafter, the same procedure was performed. Finally, the subcutaneous thigh fat thickness was measured with a skin caliper (the average of three measurements) at the location of the ultrasound probe and the accelerometer.

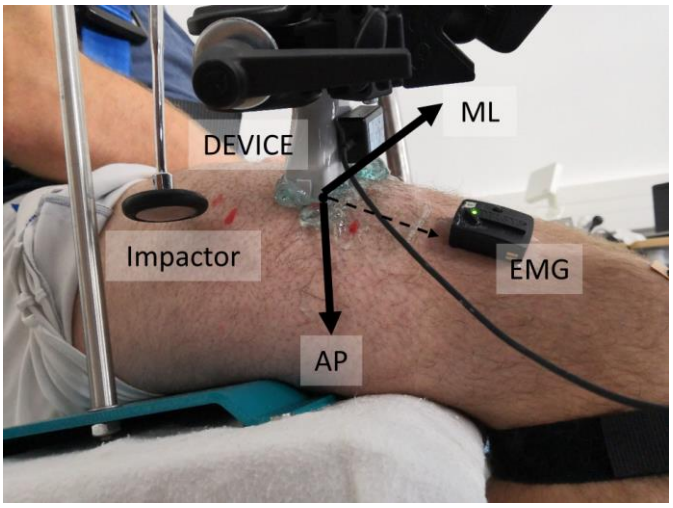

Fig. 1. Instrumentation during ultrasound measurement. ML: Medio-lateral axis; AP: Antero-posterior axis. The dashed arrow represents the longitudinal axis, orthogonal to the two others, but was not quantified in this study. DEVICE: Accelerometer or Ultrasonography.

D. Data treatment

The entire data treatment process was computed with MATLAB R2018b (MathWorks, Natick, Massachusetts, USA). Raw EMG signals of the *vastus lateralis* were run through a Butterworth bandpass filter between 10 Hz and 499 Hz. Thereafter, the root-mean-square envelope of the signal was calculated with a window length of 0.05 seconds. The signals were normalized for each participant with the mean values of the greatest 0.5-second plateau obtained during the two maximal contractions. The mean EMG was calculated from 0.5 seconds to the 0.05 seconds before the impact to avoid the noise caused by the shock [29].

Vastus lateralis accelerations were firstly computed from ultrasonographic images (bandwidth = 7.5 MHz, acquisition frequency = 1000 Hz, resolution = 256 pixels [width] x 180 pixels [height], field of view = 5 cm [width] x 2.5 cm [height]). When the *vastus lateralis* was located at the center of the image while relaxed or contracted, the upper zone of the muscles just below the subcutaneous fat was manually selected. Then, the binary robust invariant scalable keypoints (BRISK) algorithm [30], [31] was used to detect a maximum of 300 points within the selected zone. The point trajectories over time were then tracked to obtain the mediolateral and anteroposterior displacements of each point (videos are presented in supplementary files). A Butterworth bandpass filter between 10 Hz and 130 Hz was applied to the displacement of the points, and then the displacement signal was derived twice to obtain

the point acceleration in the two directions. Points with a maximum acceleration above 5 m·s^{-2} were included, and the mean acceleration of these points was analyzed. Acceleration signals from the accelerometers (i.e., the skin and probe) were filtered with a Butterworth bandpass filter between 10 Hz and 130 Hz.

Acceleration signals of the tissues assessed with ultrasonography and accelerometry in the two-dimensional axis were investigated in the time-frequency domain with a continuous wavelet transform, using a filter bank with a Morse mother wavelet with $\gamma = 3$ and $P^2 = 60$ [32]. The modulus of the coefficients produced by the wavelet transform was computed and expressed as power as a function of time and frequency, $p(t, f)$. The mean maps of the four trials for each condition and each participant were considered for analysis. Only the signal powers ranging from 10 Hz to 130 Hz during the 0.25 seconds after the impact were analyzed [6], [33]. Consequently, the power maps were composed of 30250 nodes (250 nodes [time] x 121 nodes [frequency])

Additionally, three variables (main frequency, median frequency, and damping properties) were extracted from the power maps. The energy spectrum, *E(f)*, representing the energy at each frequency, was computed by integrating the signal power of each frequency over the time interval (1):

$$E(f) = \int_{t=0}^{0.25} p(t, f)\, dt. \quad (1)$$

The main and median frequencies were computed from the energy spectrum. The main frequency corresponded to the frequency with the most energy and the median frequency to the frequency that split the spectrum into two equal parts.

The overall measured power as a function of time, *P(t)*, was computed by integrating the power with respect to the frequency (2):

$$P(t) = \int_{f=10}^{130} p(t, f)\, \mathrm{d}f. \quad (2)$$

The damping properties (*D*) were computed from the overall signal power with an optimization algorithm, which minimized the sum of the squared difference between the measured and the theoretical power decay of the vibration [12], [33]. The algorithm optimized the *D* between the instants when the power decay was maximal (T1) and when the power was equal to 10% of the power at T1 (T2) (3):

$$\min_{D} J = \sum_{t=T1}^{T2} (P_{T1} \cdot e^{-D \cdot t} - P(t))^2, \quad (3)$$

where P_{T1} is the measured power at T1, and $P_{T1} \cdot e^{-D \cdot t}$ is the theoretical power decay.

Finally, trials for which the peak acceleration of the probe of the ultrasound device was above 5 m·s^{-2} for at least one axis were excluded from the data analysis.

E. Statistics

Using the spm1d package for MATLAB [34], statistical parametric mapping (SPM) analysis was conducted in two dimensions on the power maps obtained from the wavelet transform. The SPM analysis requires a 1D-1D continuum, while power maps corresponded to a 2D-1D continuum (i.e., the power [1D] is represented as a function of time and frequency [2D]). In line with a previous study using 2D-1D SPM analysis [35], the maps were flattened into a 1D-1D continuum to allow for comparisons between the conditions and then reshaped to their original dimensions for interpretation of the results. Power maps were analyzed with a two-way analysis of variance (ANOVA) on repeated measures (i.e., *device*: accelerometer vs. ultrasound; *muscle activation level*: relaxed vs. contracted). Considering the independent analysis of the mediolateral and anteroposterior axes, the level of significance was set at 2.5% ($\alpha = 0.05/2$). Then, post hoc tests with the Bonferroni correction were performed when appropriate. To find the *F*- or *t*-value corresponding to the level of significance mentioned above, a permutation test was used. The latter is a non-parametric statistical approach consisting of permutations of the labels between the different conditions, which allows the derivation of the appropriate statistical distribution directly from the data [36]. To achieve numerical stability, the number of permutations was set at 100/α (e.g., 4000 permutations for each ANOVA).

Using R software (v3.5.0, R Core Team, Vienna, Austria), linear mixed models [37] were used to investigate the effect of the device (fixed effect) and muscular activation level (fixed effect) on the *vastus lateralis* mean EMG, main and median frequencies, and damping properties. All the trials were included in the models, and the fixed effects were set as random intercepts and slopes to adapt the model to each participant's performance. The χ^2 and p-values were obtained from likelihood ratio tests, which were conducted by testing the full model against the model without the effect tested. The alpha error (5%) was corrected with the Holm-Bonferroni method. When an interaction was observed, the two fixed effects were tested independently in each category of the other effect. Then, Tukey HSD post hoc comparisons were performed. The normality, homoscedasticity, and linearity of the linear mixed model residuals were graphically controlled.

Therewith, effect sizes (ESs) were calculated with Hedges' g for each node of the power maps and each variable. Furthermore, the ESs for the power maps were corrected for a non-normal data distribution [38].

The mean relative differences between the values obtained with accelerometry and ultrasonography were calculated for the main and median frequencies and damping properties. Linear regressions were performed between these mean relative differences and the subcutaneous fat thickness for each axis and level of activation. A total of 12 regressions were performed, and the alpha risk (5%) was corrected with the Holm-Bonferroni method. When statistically significant, correlations were classified as *strong* if Pearson's $|r|$ range was between 0.6 and 0.79 and *very strong* if greater than or equal to 0.8.

III. Results

The thigh fat thickness assessed with t
from 4 mm to 18 mm (mean ± *SD*: 9.7 :
peak accelerations of the probe in the mediolateral and anteroposterior directions were 2.1 ± 0.5 $m \cdot s^{-2}$ and 2.2 ± 0.6 $m \cdot s^{-2}$, respectively. These accelerations were, respectively, 20.3 ± 8.2 and 16.1 ± 7.0 times lower than the peak acceleration of the muscle assessed with ultrasonography. Concerning the muscular activation, linear mixed models depicted no interaction (p = 0.71, χ^2 = 0.1) or device effect (p = 0.98, χ^2 = 0.0), whereas the contracted condition led to a significantly greater mean EMG compared to the relaxed condition (p < 0.001, ES = 8.1; Fig. 2).

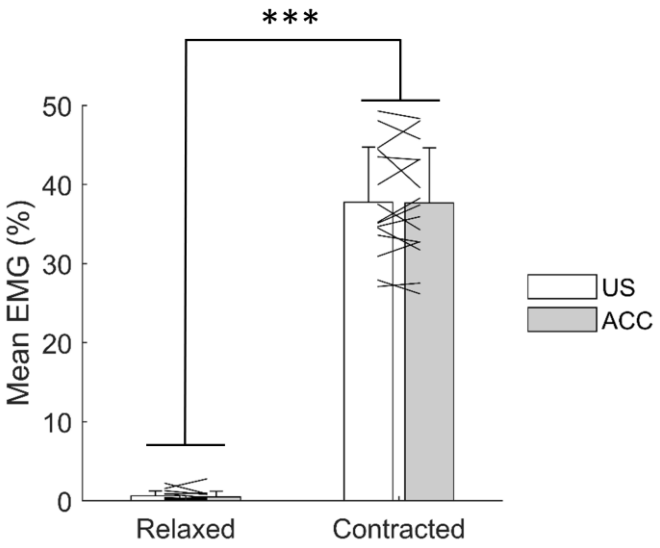

Fig. 2. Vastus lateralis *activation (mean ± SD) for the two conditions and the two devices. Black lines represent subject specific changes. US: Ultrasonography, ACC: Accelerometry. ***, p<0.001.*

A. Power map analysis

1) Mediolateral axis

The SPM ANOVA of the power maps (Fig. 3) revealed an interaction between the activation level and the device (clusters A' and C'), as well as the main effects of the device (clusters A, B_1, and B_2) and activation level (clusters C and D).

The effect of the device was observed in three clusters. Firstly, signal power between 50 Hz and 90 Hz during the first 0.06 seconds (cluster A) was 30% to 50% lower (-3 au on average) measured with accelerometry compared to ultrasonography (ES: 0.9 to 1.3). Due to an interaction effect, cluster A' was larger (up to 130 Hz) when the muscle was contracted. Secondly, cluster B may be divided into two sub-clusters. The signal power between 20 Hz and 130 Hz from 0.15 seconds (B_1) measured 150% to 250% greater (0.2 au on average) with accelerometry than with ultrasonography (ES: 2.0 to 3.0). By contrast, under 20 Hz (B_2), the signal power was 300% to 600% greater (1 au on average) when measured with accelerometry (ES: 1.4 to 1.8).

Furthermore, the effect of the activation level was represented by two distinct clusters. The first cluster (C), located between 45 Hz and 130 Hz during the first 0.1 seconds,

00% (4 au on
1.5). Due to an
ltrasonography
een 10 Hz and
20 Hz during the first 0.2 seconds and exhibited a lower power of 30% to 60% (2.5 au on average) for the contracted condition (ES: 1.2 to 2).

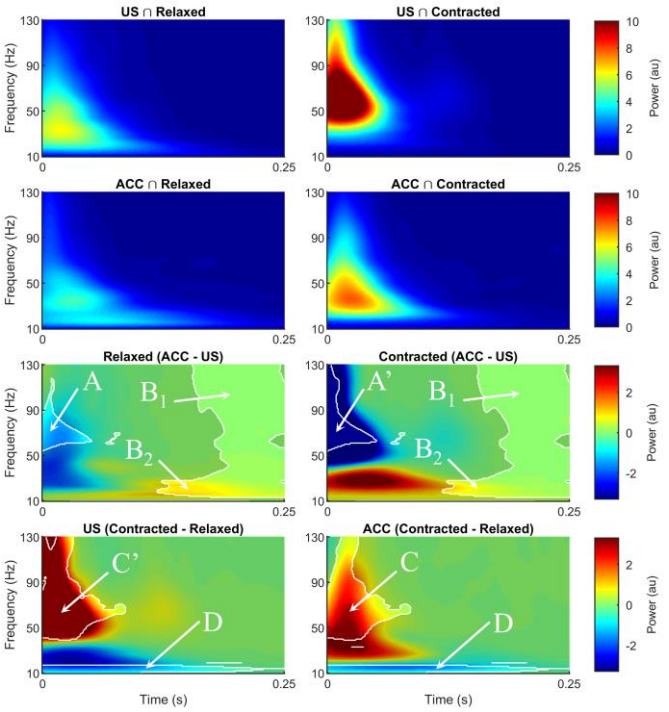

Fig. 3. From top to bottom; rows 1 and 2: mean power map for each condition of the medio-lateral axis; row 3: differences between devices for each activation condition, row 4: differences between activation conditions for each device. The enlighten clusters (A, B_1, B_2, C, and D) correspond to significant differences between two conditions. Clusters with an apostrophe (C') depicted an interaction effect within the cluster. US: Ultrasonography, ACC: Accelerometry.

2) Anteroposterior axis

The SPM ANOVA of the power maps (Fig. 4) revealed an interaction effect between the activation level and the device (clusters E', F', and G'), as well as the main effects of the device (clusters E, F, G, and H) and the activation level (clusters I and J).

The effect of the device was represented by four clusters. Firstly, from 0.05 to 0.12 seconds and between 70 Hz and 130 Hz (clusters E and E'), signal power was 40% to 60% (1 au on average) and 150% to 200% (3 au on average) greater when measured with accelerometry (ESs: 0.5 to 1.2 and 1 to 1.8) for a relaxed and contracted muscle, respectively. Secondly, power between 20 Hz and 50 Hz during the first 0.12 seconds (cluster F) was 200% to 500% (6 au on average) greater when measured with accelerometry (ES: 1.9 to 2.3). The third cluster (G) was located under 15 Hz and depicted 250% to 350% (1 au average) more power when measured with accelerometry (ES: 0.5 to 0.8). Due to an interaction effect, clusters F' and G' were larger and interrelated when the muscle was relaxed. The power between 20 Hz and 130 Hz from 0.15 seconds (cluster H) was

300% to 600% (0.2 au on average) greater when measured with accelerometry (ES: 2.0 to 4.0).

Furthermore, the effect of the activation level on the power maps was observed in two distinct clusters. The first cluster (I), between 50 Hz and 120 Hz during the first 0.12 seconds, depicted 100% to 500% (6 au) more power when the muscle was contracted (ES: 1.2 to 2.2). The second cluster (J) was located between 15 Hz and 20 Hz during the first 0.2 seconds and exhibited 30% to 60% (3 au average) less power for the contracted condition (ES: 0.8 to 1.4).

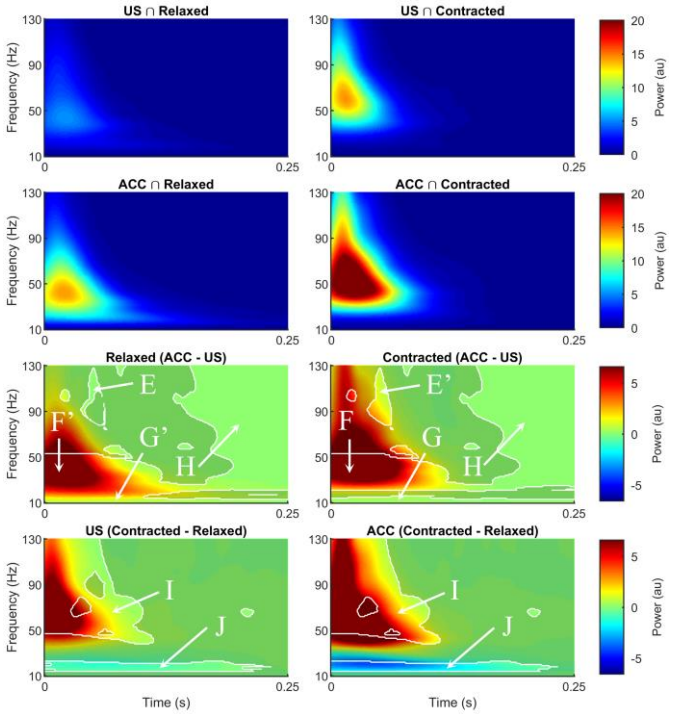

Fig. 4. From top to bottom; rows 1 and 2, mean power map for each condition of the antero-posterior axis; row 3: differences between devices for each activation condition, row 4: differences between activation conditions for each device. The enlighten clusters (E, F, G, H, I, and J) correspond to significant differences between two conditions. Clusters with an apostrophe (E', F', and G') depicted an interaction effect within the cluster. US: Ultrasonography, ACC: Accelerometry.

B. *Extracted variables*

Firstly, interaction effects on the main frequency were revealed for both axes ($p < 0.001$, $\chi^2 = 80.2$ and $p < 0.01$, $\chi^2 = 10.0$ for the mediolateral and anteroposterior axes, respectively; Table 1). Lower main frequencies were computed with accelerometry compared to ultrasonography, more significantly for a contracted muscle than for a relaxed one (-49%, $p < 0.001$, ES = 3.9 compared to -35%, $p < 0.001$, ES = 1.5 and -18%, $p < 0.01$, ES = 1.2 compared to -13%, $p < 0.01$, ES = 0.6 for the mediolateral and anteroposterior axes, respectively). Moreover, higher main frequencies were observed when the muscle was contracted than relaxed, though less significantly when quantified with accelerometry rather than ultrasonography (+50%, $p < 0.001$, ES = 1.6 compared to +93%, $p < 0.001$, ES = 3.5 and +46%, $p < 0.001$, ES = 1.6 compared to +53%, $p < 0.001$, ES = 2.5 for the mediolateral and anteroposterior axes, respectively).

Secondly, interaction effects were revealed for the mediolateral axis on the median frequency ($p < 0.001$, $\chi^2 = 102.6$; Table 1). Lower median frequencies were observed when quantified with accelerometry than with ultrasonography, more significantly for a contracted muscle than for a relaxed one (-38%, $p < 0.001$, ES = 4.1 compared to -20%, $p < 0.001$, ES = 1.2). Higher frequencies were observed for a contracted muscle than for a relaxed one, less significantly when quantified with accelerometry compared to ultrasonography (+25%, $p < 0.001$, ES = 2.2 compared to +44%, $p < 0.001$, ES = 3.3). Additionally, for the anteroposterior axis, only the main effects of the activation level and device were found (Table 1). Lower median frequencies were quantified with accelerometry compared to ultrasonography (-14%, $p < 0.001$, ES = 0.9), and higher frequencies were observed when the muscle was contracted rather than relaxed (+29%, $p < 0.001$, ES = 2.1).

Finally, the main effects of the activation level and device on the damping properties were calculated (Table 1). Reduced damping properties were found when quantified with accelerometry compared to ultrasonography (-37%, $p < 0.001$, ES = 1.4 and -15%, $p < 0.01$, ES = 0.7 for the mediolateral and anteroposterior axes, respectively). Greater damping properties were observed for a contracted muscle compared to a relaxed one (+66%, $p < 0.001$, ES = 1.6 and +14%, $p < 0.01$, ES = 0.6 for the mediolateral and anteroposterior axes, respectively).

TABLE I
VIBRATIONS CHARACTERISTICS

Variables	Axes	US ∩ Relaxed	ACC ∩ Relaxed	US ∩ Contracted	ACC ∩ Contracted
Main Frequency (Hz)	ML	28.3 ± 8.1 *	18.5 ± 4.6	54.6 ± 6.8 #$	27.7 ± 7.0 *
	AP	35.4 ± 7.9 *	30.7 ± 8.4	54.2 ± 7.0 #$	44.7 ± 8.6 *
Median Frequency (Hz)	ML	42.5 ± 6.5 *	35.6 ± 4.4	61.2 ± 4.5 #$	44.4 ± 3.7 *
	AP	49.6 ± 4.8 *	42.2 ± 5.5	63.5 ± 5.2 #$	55.4 ± 5.4 *
Damping (/s)	ML	25.7 ± 7.5 *	14.9 ± 3.4	40.7 ± 5.8 #$	26.7 ± 4.8 *
	AP	34.5 ± 4.0 *	30.3 ± 6.5	40.4 ± 9.9 #$	33.5 ± 7.6 *

Mean ± SD of the main, median frequencies and damping. US: Ultrasonography; ACC: Accelerometry. ML: medio-lateral axis; AP: antero-posterior axis. * means different of ACC ∩ Relaxed; # for different of US ∩ Relaxed; $ when different of ACC ∩ Contracted.

C. *Correlation with thigh fat thickness*

Significant correlations were found for the anteroposterior axis (Fig.5). For an increase of 1 mm of subcutaneous fat, the relative difference of the main frequency between ultrasonography and accelerometry increased on average by 3.4% for a contracted muscle (*strong*). The relative differences for the median frequency between the two devices also increased on average by 2.4% and 1.7% per 1 mm of fat thickness for a relaxed (*very strong*) and contracted (*strong*) muscle, respectively. The relative differences in damping

properties increased on average by 3.4% per 1 mm of fat for a relaxed muscle (*very strong*).

IV. Discussion

The purpose of this study was to determine whether a skin-mounted accelerometer reflects muscle vibrations assessed with ultrafast ultrasonography in a relaxed and contracted muscle. Compared to the ultrasound, the accelerometer overestimated the muscle vibration power under 20 Hz at the end of the vibration and underestimated the muscle vibration power above 50 Hz during the first 0.06 seconds after an impact for both the relaxed and contracted conditions. These discrepancies made the accelerometer underestimate the main and median frequencies, as well as the damping properties of the muscle. Furthermore, the differences observed between the two devices were greater when thigh fat thickness increased.

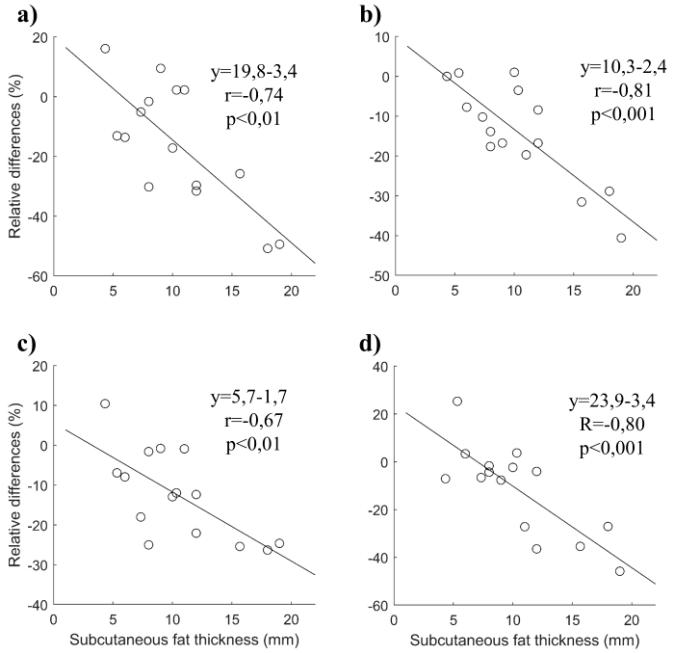

Fig. 5. Linear correlations between the subcutaneous fat thickness and the mean relative differences among accelerometry and ultrasonography on the antero-posterior axis for a) the main frequency on a contracted muscle, b) the median frequency for a relaxed and c) for a contracted muscle, d) the damping properties on a relaxed muscle.

A. Methodological considerations

To better characterize muscle behavior after an external impact, some methodological choices were made. Considering that a muscle tends to damp the vibrations as soon as an impact is initiated [3], the location of the probe and accelerometer with respect to the muscle belly had to be the same when comparing the measurement methods. Consequently, the recordings could not be performed simultaneously with the two devices. Therefore, precautions were taken to ensure that the two measurements were performed on the same location under uniform conditions. To that end, the mean muscular activation had to be similar when vibrations were recorded with either accelerometry or ultrasonography. We also ensured that vibrations generated by the impactor were minimally transmitted to the ultrasound probe during ultrasonographic measurement.

Different factors were considered in analyzing the ultrasound imaging videos. Our tracking method differed from previous studies aimed at tracking vibrations with ultrasound videos [26], [27]. As the muscle does not behave like a rigid body, a sliding window was not suitable for our purpose. Likewise, previous analysis of the data indicated that corner detection methods such as the Kanade-Lucas-Tomasi algorithm were not optimal, as the points tracked often disappeared during maximal amplitude acceleration. Thus, the BRISK algorithm [30] for detecting features (i.e., corners and the zones around them) appeared to be more appropriate. Furthermore, as the shockwave did not travel through all the points tracked, some points remained motionless over time. Therefore, a minimum limit of 5 $m \cdot s^{-2}$ was set to ensure that only the points undergoing vibration were included in the computation of average acceleration.

Consequently, the acceleration signals obtained from the ultrasound videos were considered to reflect the vibrations of the muscle only and not those of the other soft tissues.

B. Bias induced by superficial tissues

The extracted variables quantified with accelerometry aligned with a previous study reporting that the soft tissue vibrations of the *vastus lateralis* induced by an impactor have a main frequency ranging from 10 Hz to 40 Hz and damping properties from 10 s^{-1} to 60 s^{-1} for a relaxed and fully activated muscle, respectively [1]. However, these values were lower than those obtained from the muscle with ultrasonographic measurement. The power map analysis revealed that superficial tissues biased the vibration signal of the muscle by amplifying the power under 20 Hz and attenuating it above 50 Hz when estimated with accelerometry. The additional power observed with the accelerometer under 20 Hz at the end of the vibration may be explained by the lower stiffness and damping properties of the superficial tissues [25]. On the contrary, the lower power observed with the accelerometer above 50 Hz just after the impact may be the consequence of the superficial tissues acting like a low-pass filter [25]. Furthermore, we observed that an increase in the fat thickness intensifies the underestimation of the frequency content and damping properties of the muscle vibrations. This outcome aligns with the map analyses; on one hand, a lower power above 50 Hz causes a lower median frequency, and on the other hand, a greater power under 20 Hz at the end of the vibration involves decreased damping properties and a lower main frequency. Other differences in power at the end of the vibration and above 20 Hz were observed. These differences were small (0.2 au) relative to the total vibration power and may correspond to signal noise.

Similarly to a previous study [1], increasing muscular activation led to increased damping properties and higher main and median frequencies. More specifically, the increase in the frequency content from the relaxed to contracted muscle was greater when observed with ultrasonography compared to accelerometry. As discussed above, these discrepancies may be explained by the superficial tissues amplifying energy under 20 Hz and attenuating energy above 50 Hz. Thus, the

superficial tissues decrease the sensitivity of the accelerometer to capture changes in vibration characteristics between a relaxed and contracted muscle, especially when the subcutaneous fat is thicker

Accurate characterization of muscle vibrations could engender a better understanding of the muscle tuning paradigm [7], help in assessing muscle properties [1], and clarify the effects of fatigue or sports equipment on soft tissue vibration characteristics [15]. For instance, previous studies indicated that little or none of the energy of the input localized above 50 Hz was transmitted to the soft tissues [2], [39]. This result might be due to the underestimation of the vibration power above this limit by the accelerometer. Thus, muscles might vibrate at frequencies above 50 Hz during activities like running. Moreover, some authors have defined damping properties as the work performed by the muscle to damp vibration [5], [7]. Hence, the underestimation of damping when measured with an accelerometer may lead to an underestimation of the work performed by the muscle.

C. Practical applications

The use of accelerometry during sports activities is the most applicable method for soft tissue vibration assessment outside a laboratory. Despite some under- and over-estimations, accelerometry can reflect the effects of muscular activation and can be used to detect differences in frequency content or damping during sports activities. However, our results indicate that accelerometers should be used with caution, and some suggestions are proposed for using the full potential of accelerometry. Firstly, a muscle contracted at 40% vibrates at a higher frequency than the superficial tissues. In this case, a 20-Hz high-pass filtering of the signal can remove some artifacts caused by the superficial tissues vibrating at a frequency below 20 Hz. However, as a relaxed muscle vibrates at a frequency around 20 Hz, this filter may also remove some muscle vibrations and, therefore, should not be used. Secondly, the inclusion of subjects with thinner subcutaneous fat tissue can limit the under- and over-estimation of the power induced by the accelerometry method at some frequencies. Quantification of the subcutaneous fat thickness under the location of each accelerometer is recommended, especially when comparisons between individuals are performed (e.g., men vs. women). Since our experimental protocol was not designed to develop correction algorithms for the accelerometry signal, further studies are needed to address this issue.

D. Limitations

The results in the present study were obtained after an administered shock to the lateral part of the *vastus lateralis* muscle, which may differ from values recorded during sports activities, as the amplitude of the vibrations was smaller than in running or landing [39]. Furthermore, only the upper zone of the *vastus lateralis* muscle was studied, and our outcomes may not be inferred to other muscles. Moreover, as the muscle damps the vibrations along its fibers, further explorations are needed to determine the effect of the spatial location of the measuring device on the findings of the present study.

All measurements were firstly performed with ultrasonography and then with accelerometry. No randomization between the conditions could have been made, as the ultrasonography measurement had to be completed before the accelerometry measurement to determine the zone of interest. However, contractions were submaximal, and a rest period was allowed between each shock; thus, the first measurements should not alter the rest of the experiment.

V. Conclusion

The comparison between skin-mounted accelerometry and ultrafast ultrasonography revealed that the accelerometer exhibited limitations in accurately assessing muscle vibrations. More precisely, superficial tissues modify the acceleration signal when quantified by accelerometry compared to ultrasonography, by amplifying the vibration power under 20 Hz and attenuating it above 50 Hz. Moreover, when the subcutaneous fat was thicker, the underestimation of the damping properties and vibration frequency was greater. Consequently, accelerometry seems to be an appropriate method to depict the salient characteristics of muscle vibrations; however, the outcomes should be considered cautiously with respect to fat thickness. Further studies are needed to develop correction algorithms for muscle vibrations estimated with accelerometry, especially during sports activities.

VI. Conflict of interest statement

The authors declare no conflict of interest.

References

[1] J. M. Wakeling and B. M. Nigg, “Modification of soft tissue vibrations in the leg by muscular activity,” *J. Appl. Physiol.*, vol. 90, no. 2, pp. 412–420, 2001.

[2] J. M. Wakeling, B. M. Nigg, and A. I. Rozitis, “Muscle activity damps the soft tissue resonance that occurs in response to pulsed and continuous vibrations,” *J. Appl. Physiol.*, vol. 93, no. 3, pp. 1093–1103, Sep. 2002, doi: 10.1152/japplphysiol.00142.2002.

[3] K. A. Boyer and B. M. Nigg, “Soft tissue vibrations within one soft tissue compartment,” *J. Biomech.*, vol. 39, no. 4, pp. 645–651, Jan. 2006, doi: 10.1016/j.jbiomech.2005.01.027.

[4] K. A. Boyer and B. M. Nigg, “Changes in Muscle Activity in Response to Different Impact Forces Affect Soft Tissue Compartment Mechanical Properties,” *J. Biomech. Eng.*, vol. 129, no. 4, p. 594, 2007, doi: 10.1115/1.2746384.

[5] H. Enders, V. von Tscharner, and B. M. Nigg, “The effects of preferred and non-preferred running strike patterns on tissue vibration properties,” *J. Sci. Med. Sport*, vol. 17, no. 2, pp. 218–222, Mar. 2014, doi: 10.1016/j.jsams.2013.03.015.

[6] A. Khassetarash, R. Hassannejad, H. Enders, and M. M. Ettefagh, “Damping and energy dissipation in soft tissue vibrations during running,” *J. Biomech.*, vol. 48, no. 2, pp. 204–209, Jan. 2015, doi: 10.1016/j.jbiomech.2014.11.051.

[7] B. M. Nigg and J. M. Wakeling, “Impact forces and muscle tuning: a new paradigm,” *Exerc. Sport Sci. Rev.*, vol. 29, no. 1, pp. 37–41, 2001.

[8] B. M. Nigg and W. Liu, “The effect of muscle stiffness and damping on simulated impact force peaks during running,” *J. Biomech.*, vol. 32, no. 8, pp. 849–856, 1999.

[9] J. M. Wakeling, A.-M. Liphardt, and B. M. Nigg, “Muscle activity reduces soft-tissue resonance at heel-strike during walking,” *J. Biomech.*, vol. 36, no. 12, pp. 1761–1769, Dec. 2003, doi: 10.1016/S0021-9290(03)00216-1.

[10] K. A. Boyer, “Muscle Tuning During Running: Implications of an Un-tuned Landing,” *J. Biomech. Eng.*, vol. 128, no. 6, p. 815, Jun. 2006, doi: 10.1115/1.2354202.

[11] K. A. Boyer and B. M. Nigg, “Muscle activity in the leg is tuned in response to impact force characteristics,” *J. Biomech.*, vol. 37, no. 10, pp. 1583–1588, Oct. 2004, doi: 10.1016/j.jbiomech.2004.01.002.

[12] A. Martínez, C. K.-Y. Lam, V. von Tscharner, and B. M. Nigg, “Soft tissue vibration dynamics after an unexpected impact,” *Physiol. Rep.*, vol. 7, no. 2, p. e13990, Jan. 2019, doi: 10.14814/phy2.13990.

[13] B. Friesenbichler, L. M. Stirling, P. Federolf, and B. M. Nigg, “Tissue vibration in prolonged running,” *J. Biomech.*, vol. 44, no. 1, pp. 116–120, Jan. 2011, doi: 10.1016/j.jbiomech.2010.08.034.

[14] A. Khassetarash, R. Hassannejad, M. M. Ettefagh, and V. Sari-Sarraf, “Fatigue and soft tissue vibration during prolonged running,” *Hum. Mov. Sci.*, vol. 44, pp. 157–167, Dec. 2015, doi: 10.1016/j.humov.2015.08.024.

[15] S. Ehrström, M. Gruet, M. Giandolini, S. Chapuis, J.-B. Morin, and F. Vercruyssen, “Acute and Delayed Neuromuscular Alterations Induced by Downhill Running in Trained Trail Runners: Beneficial Effects of High-Pressure Compression Garments,” *Front. Physiol.*, vol. 9, Nov. 2018, doi: 10.3389/fphys.2018.01627.

[16] W. Fu, Y. Liu, and S. Zhang, “Effects of Footwear on Impact Forces and Soft Tissue Vibrations during Drop Jumps and Unanticipated Drop Landings,” *Int. J. Sports Med.*, vol. 34, no. 06, pp. 477–483, Nov. 2012, doi: 10.1055/s-0032-1327696.

[17] W. Fu, X. Wang, and Y. Liu, “Impact-induced soft-tissue vibrations associate with muscle activation in human landing movements: An accelerometry and EMG evaluation,” *Technol. Health Care*, vol. 23, no. s2, pp. S179–S187, Jun. 2015, doi: 10.3233/THC-150952.

[18] W. Fu, Y. Fang, Y. Gu, L. Huang, L. Li, and Y. Liu, “Shoe cushioning reduces impact and muscle activation during landings from unexpected, but not self-initiated, drops,” *J. Sci. Med. Sport*, vol. 20, no. 10, pp. 915–920, Oct. 2017, doi: 10.1016/j.jsams.2017.03.009.

[19] R. Trama, Y. Blache, and C. Hautier, “Effect of rocker shoes and running speed on lower limb mechanics and soft tissue vibrations,” *J. Biomech.*, vol. 82, pp. 171–177, Jan. 2019, doi: 10.1016/j.jbiomech.2018.10.023.

[20] F. Hintzy, N. Gregoire, P. Samozino, X. Chiementin, W. Bertucci, and J. Rossi, “Effect of thigh-compression shorts on muscle activity and soft tissue vibration during cycling.:,” *J. Strength Cond. Res.*, p. 1, Dec. 2017, doi: 10.1519/JSC.0000000000002402.

[21] M. Giandolini, M. Munera, X. Chiementin, S. Bartold, and N. Horvais, “Footwear influences soft-tissue vibrations in rearfoot strike runners,” *Footwear Sci.*, vol. 9, no. sup1, pp. S25–S27, Jun. 2017, doi: 10.1080/19424280.2017.1313902.

[22] L. Necking, L. Dahlin, J. Friden, G. Lundborg, R. Lundstrom, and L. Thornell, “Vibration-induced muscle injury An experimental model and preliminary findings,” *J. Hand Surg. J. Br. Soc. Surg. Hand*, vol. 17, no. 3, pp. 270–274, Jun. 1992, doi: 10.1016/0266-7681(92)90113-G.

[23] M. de Hoyo *et al.*, “Impact of an acute bout of vibration on muscle contractile properties, creatine kinase and lactate dehydrogenase response,” *Eur. J. Sport Sci.*, vol. 13, no. 6, pp. 666–673, Nov. 2013, doi: 10.1080/17461391.2013.774052.

[24] J. Rittweger, M. Mutschelknauss, and D. Felsenberg, “Acute changes in neuromuscular excitability after exhaustive whole body vibration exercise as compared to exhaustion by squatting exercise,” *Clin. Physiol. Funct. Imaging*, vol. 23, no. 2, pp. 81–86, 2003.

[25] J. E. Smeathers, “Transient vibrations caused by heel strike,” *Proc. Inst. Mech. Eng. Part H*, vol. 203, no. 4, pp. 181–186, 1989, doi: 10.1243/PIME_PROC_1989_203_036_01.

[26] T. Kaddoura, A. Au, G. Kawchuk, R. Uwiera, R. Fox, and R. Zemp, “Non-invasive spinal vibration testing using ultrafast ultrasound imaging: A new way to measure spine function,” *Sci. Rep.*, vol. 8, no. 1, p. 9611, Dec. 2018, doi: 10.1038/s41598-018-27816-0.

[27] D. Yamada, A. Degirmenci, and R. Howe, “Ultrasound Imaging for Identifying Dynamics of Soft Tissue,” *IEEE 15th Int. Symp. Biomed. Imaging ISIB 2018*, pp. 1161–1165, Apr. 2018.

[28] H. J. Hermens, B. Freriks, C. Disselhorst-Klug, and G. Rau, “Development of recommendations for SEMG sensors and sensor placement procedures,” *J. Electromyogr. Kinesiol.*, vol. 10, no. 5, pp. 361–374, Oct. 2000, doi: 10.1016/S1050-6411(00)00027-4.

[29] A. Fratini, M. Cesarelli, P. Bifulco, and M. Romano, “Relevance of motion artifact in electromyography recordings during vibration treatment,” *J. Electromyogr. Kinesiol.*, vol. 19, no. 4, pp. 710–718, Aug. 2009, doi: 10.1016/j.jelekin.2008.04.005.

[30] S. Leutenegger, M. Chli, and R. Y. Siegwart, “BRISK: Binary Robust invariant scalable keypoints,” in *2011 International Conference on Computer Vision*, Barcelona, Spain, Nov. 2011, pp. 2548–2555, doi: 10.1109/ICCV.2011.6126542.

[31] S. A. K. Tareen and Z. Saleem, “A comparative analysis of SIFT, SURF, KAZE, AKAZE, ORB, and BRISK,” in *2018 International Conference on Computing, Mathematics and Engineering Technologies (iCoMET)*, Sukkur, Mar. 2018, pp. 1–10, doi: 10.1109/ICOMET.2018.8346440.

[32] J. M. Lilly and S. C. Olhede, “Higher-Order Properties of Analytic Wavelets,” *IEEE Trans. Signal Process.*, vol. 57, no. 1, pp. 146–160, Jan. 2009, doi: 10.1109/TSP.2008.2007607.

[33] H. Enders, V. von Tscharner, and B. M. Nigg, “Analysis of damped tissue vibrations in time-frequency space: a wavelet-based approach,” *J. Biomech.*, vol. 45, no. 16, pp. 2855–2859, Nov. 2012, doi: 10.1016/j.jbiomech.2012.08.027.

[34] T. C. Pataky, “Generalized n-dimensional biomechanical field analysis using statistical parametric mapping,” *J. Biomech.*, vol. 43, no. 10, pp. 1976–1982, Jul. 2010, doi: 10.1016/j.jbiomech.2010.03.008.

[35] T. C. Pataky, “Spatial resolution in plantar pressure measurement revisited,” *J. Biomech.*, vol. 45, no. 12, pp. 2116–2124, Aug. 2012, doi: 10.1016/j.jbiomech.2012.05.038.

[36] T. E. Nichols and A. P. Holmes, “Nonparametric permutation tests for functional neuroimaging: A primer with examples,” *Hum. Brain Mapp.*, vol. 15, no. 1, pp. 1–25, Jan. 2002, doi: 10.1002/hbm.1058.

[37] D. Bates, M. Mächler, B. Bolker, and S. Walker, “Fitting Linear Mixed-Effects Models Using lme4,” *J. Stat. Softw.*, vol. 67, no. 1, pp. 1–48, 2015, doi: 10.18637/jss.v067.i01.

[38] K. Kelley, “The Effects of Nonnormal Distributions on Confidence Intervals Around the Standardized Mean Difference: Bootstrap and Parametric Confidence Intervals,” *Educ. Psychol. Meas.*, vol. 65, no. 1, pp. 51–69, Feb. 2005, doi: 10.1177/0013164404264850.

[39] R. Trama, C. Hautier, and Y. Blache, “Input and Soft-Tissue Vibration Characteristics during Sport-Specific Tasks:,” *Med. Sci. Sports Exerc.*, p. 1, Jul. 2019, doi: 10.1249/MSS.0000000000002106.